AFRL-RX-WP-TP-2011-4295

REFRACTORY HIGH-ENTROPY ALLOYS (PREPRINT)

O.N. Senkov

UES, Inc.

D.B. Miracle

Metals Branch
Metals, Ceramics, and NDE Division

G.B. Wilks

General Dynamics Corporation

C.P. Chuang and P.K. Liaw

The University of Tennessee

JULY 2011

STINFO COPY

AIR FORCE RESEARCH LABORATORY
MATERIALS AND MANUFACTURING DIRECTORATE
WRIGHT-PATTERSON AIR FORCE BASE, OH 45433-7750
AIR FORCE MATERIEL COMMAND
UNITED STATES AIR FORCE

REPORT DOCUMENTATION PAGE

1. REPORT DATE *(DD-MM-YY)*	2. REPORT TYPE	3. DATES COVERED *(From - To)*
July 2011	Journal Article Preprint	01 July 2011 – 01 July 2011

4. TITLE AND SUBTITLE
THE DUALITY OF FRACTURE BEHAVIOR IN A Ca-BASED BULK-METALLIC GLASS (PREPRINT)

5a. CONTRACT NUMBER
In-house

5b. GRANT NUMBER

5c. PROGRAM ELEMENT NUMBER
62102F

6. AUTHOR(S)
O.N. Senkov (UES, Inc.)
D.B. Miracle (AFRL/RXLM)
G.B. Wilks (General Dynamics Corporation)
C.P. Chuang and P.K. Liaw (The University of Tennessee)

5d. PROJECT NUMBER
4347

5e. TASK NUMBER
20

5f. WORK UNIT NUMBER
LM10512P

7. PERFORMING ORGANIZATION NAME(S) AND ADDRESS(ES)
UES, Inc.
Dayton, OH 45432-1894

Metals Branch (AFRL/RXLM)
Metals, Ceramics, and NDE Division
Air Force Research Laboratory, Materials and
Manufacturing Directorate
Wright-Patterson Air Force Base, OH 45433-7750
Air Force Materiel Command, United States Air Force

General Dynamics Corporation
Dayton, OH 45431

The University of Tennessee
Department of Materials Science and
 Engineering
Knoxville, TN 37996

8. PERFORMING ORGANIZATION REPORT NUMBER
AFRL-RX-WP-TP-2011-4295

9. SPONSORING/MONITORING AGENCY NAME(S) AND ADDRESS(ES)
Air Force Research Laboratory
Materials and Manufacturing Directorate
Wright-Patterson Air Force Base, OH 45433-7750
Air Force Materiel Command
United States Air Force

10. SPONSORING/MONITORING AGENCY ACRONYM(S)
AFRL/RXLM

11. SPONSORING/MONITORING AGENCY REPORT NUMBER(S)
AFRL-RX-WP-TP-2011-4295

12. DISTRIBUTION/AVAILABILITY STATEMENT
Approved for public release; distribution unlimited.

13. SUPPLEMENTARY NOTES

14. ABSTRACT
Two refractory alloys, W-Nb-Mo-Ta and W-Nb-Mo-Ta-V, with near-equiatomic compositions were produced by vacuum arc-melting. Both alloys have a single-phase body-centered cubic (BCC) structure. The lattice parameters $a = 3.2134$ Å for the quaternary alloy and $a = 3.1832$ Å for the quinternary alloy were determined with the use of a high-energy X-ray diffraction and the scattering vector length range from 0.7 to 20 A^{-1}. The alloy density and Vickers microhardness were $\rho = 13.75$ g/cm^3 and $H_v = 4455$ MPa for the W-Nb-Mo-Ta alloy and $\rho = 12.36$ g/cm^3 and $H_v = 5250$ MPa for the W-Nb-Mo-Ta-V alloy. The higher microhardness was related to the finer grain structure in the quinternary alloy.

15. SUBJECT TERMS
refractory alloys, near-equiatomic compositions, vacuum arc-melting, Metallic alloys

16. SECURITY CLASSIFICATION OF:			17. LIMITATION OF ABSTRACT:	18. NUMBER OF PAGES	19a. NAME OF RESPONSIBLE PERSON (Monitor)
a. REPORT	**b. ABSTRACT**	**c. THIS PAGE**	SAR	22	Jonathan E. Spowart
Unclassified	Unclassified	Unclassified			**19b. TELEPHONE NUMBER** *(Include Area Code)* N/A

REFRACTORY HIGH-ENTROPY ALLOYS

O.N. Senkov[1,2,*], D.B. Miracle[1], G.B. Wilks[1,3], C.P. Chuang[4], P.K. Liaw[4]

[1] Air Force Research Laboratory, Materials and Manufacturing Directorate, Wright-Patterson Air Force Base, OH 45433, USA

[2] UES, Inc., Dayton, OH 45432, USA

[3] General Dynamics Corporation, Dayton, OH 45431, USA

[4] Department of Material Science and Engineering, the University of Tennessee, Knoxville, TN 37996, USA

ABSTRACT

Two refractory alloys, W-Nb-Mo-Ta and W-Nb-Mo-Ta-V, with near-equiatomic compositions were produced by vacuum arc-melting. Both alloys have a single-phase body-centered cubic (BCC) structure. The lattice parameters $a = 3.2134$ Å for the quaternary alloy and $a = 3.1832$ Å for the quinternary alloy were determined with the use of a high-energy X-ray diffraction and the scattering vector length range from 0.7 to 20 A^{-1}. The alloy density and Vickers microhardness were $\rho = 13.75$ g/cm^3 and $H_v = 4455$ MPa for the W-Nb-Mo-Ta alloy and $\rho = 12.36$ g/cm^3 and $H_v = 5250$ MPa for the W-Nb-Mo-Ta-V alloy. The higher microhardness was related to the finer grain structure in the quinternary alloy.

INTRODUCTION

Metallic alloys with superior mechanical and functional properties remain in high demand for the aerospace industry. Conventional metal alloys, especially for structural applications, are sometimes considered a relatively mature technology with a long history and only evolutionary scope for improvement. However, conventional metal alloys represent only a narrow range of possibilities. Conventional metal alloys usually have a base element that dominates the chemistry, accounting for ~80% (weight percent) or more of the total formulation. Superalloys, with as many as 12 elements in a single alloy, still typically contain over 50% of a base element. In some cases, superalloys with roughly 20% each of up to three transition metal elements (Fe, Ni, Co, Cr) have also been developed and used. Many reasons can be suggested to rationalize this limited scope in alloying strategy. It is sometimes found that ternary or higher-order

* Corresponding author. Phone: 937-2551320, e-mail: oleg.senkov@wpafb.af.mil

intermetallic compounds form unexpectedly in multi-component alloys, generally after long-term exposure at elevated operating temperatures. These new phases often have complex crystal structures that do not support plasticity, and they scavenge desirable elements from the host alloy. Formation of these complex intermetallics typically heralds a reduction in mechanical properties, reduced corrosion resistance and microstructural instability. This long-held experience provides a strong disincentive for unnecessarily complex alloy formulations. Within the past several years, a fundamentally new alloying concept has been proposed [1,2,3]. In this approach, multi-component alloys are formed with n elements *of roughly equi-molar concentrations*. When n is large (typically $n > 5$), the high entropy of mixing can stabilize solid solution phases with relatively simple crystal structures rather than forming complex intermetallic phases. Thus, while these alloys may be compositionally complex, they are microstructurally simple. Termed multicomponent high entropy alloys, or simply high entropy alloys (HEAs), this concept offers a new opportunity to explore, discover and develop fundamentally new classes of alloys for structural and functional applications. The opportunities for new alloy discovery are vast. Alloying element combinations that were previously objectionable due to microstructural instability may now be a possibility, suggesting completely new families of light metal alloys, high strength metals and high temperature metals for load-bearing structures and thermal protection.

In this paper, development and analysis of two refractory high-density HEAs, W-Nb-Mo-Ta and W-Nb-Mo-Ta-V, are reported.

EXPERIMENTAL PROCEDURES

The W-Nb-Mo-Ta and W-Nb-Mo-Ta-V alloys were prepared at Pittsburgh Materials Technology, Inc. (Jefferson Hills, PA) by vacuum arc melting of the equimolar mixtures of the corresponding elements. High purity titanium was used as a getter for residual gases in the high vacuum chamber. The tungsten, molybdenum and vanadium were in the form of 45.7 mm diameter rods with a purity of 99.7%, 99.0% and 99.9%, respectively. The tantalum and niobium were in the form of chips and had a purity of 99.0% and 99.99%, respectively. The alloys were prepared in the form of buttons of ~ 10 mm thickness and ~60-70 mm in diameter. To achieve homogeneous distribution of elements in the alloys, the buttons were re-melted four times, were flipped for each melt, and had a total time of over 1 hour in liquid state. The buttons had shiny surfaces indicating no oxidation during vacuum arc melting. The final actual composition of the alloys, which was obtained using inductively-coupled plasma-optical emission spectroscopy (ICP-OES), is given in

Table 1. It can be noticed that the composition is slightly off of the equiatomic composition. The microstructure and properties of the alloys were studied in the as-cast condition. The crystal structure was identified with the use of a high-energy synchrotron X-ray diffraction (the MAR345 Image Plate Detector, Advanced Photon Source, Argonne National Laboratory). The samples for the X-ray diffraction were in the form of ~0.75 mm thick plates. The X-ray energy was 105 keV and the beam cross-section was 0.05 x 0.05 mm. The scattering vector length $Q = 4\pi\sin\Theta/\lambda$, where λ is an X-ray of wavelength and 2Θ is the scattering angle, was in the range from 0.7 to 20 A^{-1}.

The density of the alloys was measured with an AccuPyc 1330 V1.03 pycnometer. The pycnometer cell volume was 12.2284 cm^3, the weight of the samples was from 10 to 15 g and was measured with accuracy of ±0.0001 g, and the volume of the samples was determined with the accuracy of ±0.0001 cm^3 by measurement of the free volume of the loaded cell using the helium gas and ten purges.

The microstructure was analyzed with the use of a scanning electron microscope equipped with the backscatter electron (BSE) detector and energy dispersive spectroscopy (EDS) analysis detector. Electron probe micro-analysis (EPMA) was conducted using a Cameca SX100 micro-analyzer operating at the accelerating voltage of 15 keV. The effective excitation volume at the sample surface, from which the elemental composition was collected, was ~ 3 μm in diameter and ~ 3 μm deep. Vickers microhardness was measured on polished cross-section surfaces using a 136-degree Vickers diamond pyramid under 500 g load applied for 30 seconds.

RESULTS AND DISCUSSIONS

Crystal Structure

Figures 1a and 1b show X-ray diffraction patterns of the studied refractory high entropy alloys. In these figures, Q is plotted versus the scattered X-ray intensity. The inter-planar spacing *d* is related to Q through the formula:

$d = 2\pi/Q = \lambda/(2\sin\Theta)$ (1)

All peaks on these X-ray patterns have been identified to belong to a BCC phase and the indexes of the crystal planes corresponding to the X-ray diffraction peaks are shown in the figures. The

lattice parameters a_1 = 3.2134 Å and a_2 = 3.1832 Å was calculated from these diffraction patterns for Alloy1 and Alloy 2, respectively. The different relative intensities of the same peaks in two alloys were probably due to the apparent texture effects caused by small amounts of grains within the X-ray excited volume.

It is necessary to point out that all five elements used to produce these two alloys have the BCC crystal lattices. The lattice parameters of these pure metals, taken from [4] are given in Table 2. Using the rule of mixture, the 'theoretical' crystal lattice parameter a_{mix} of an alloy can be calculated using Equation (2):

$$a_{mix} = \sum c_i a_i \tag{2}$$

where c_i and a_i are the atomic fraction and the lattice parameter of element i. The calculated a_{mix} for the studied alloys are given in Table 2. The experimental a values, determined by X-ray diffraction are also given in this table. It can be seen that, within an experimental error, the lattice parameter of Alloy 2 follows the rule of mixture. This may indicate that the BCC phase is a fully disordered solid solution in this alloy. On the other hand, the calculated lattice parameter of Alloy 1 is about 0.3% larger than the experimentally measured, which may indicate some solution ordering in this quaternary alloy. The solid solution ordering can also be responsible for the absence of peaks from the crystallographic planes (222), (800), (660), (822), (840), and (664) in Alloy 1, though these peaks are present on the X-ray diffraction pattern of Alloy 2.

Alloy Density

The densities of the alloys were determined to be ρ_1 = 13.75 ± 0.028 g/cm^3 for the W-Nb-Mo-Ta alloy and ρ_2 = 12.36 ± 0.011 g/cm^3 for the W-Nb-Mo-Ta-V alloy (see Table 2). This density values can be compared with theoretical density of disordered solid solution, ρ_{theor}, which is given by Equation (3):

$$\rho_{theor} = \frac{\sum c_i A_i}{\sum \dfrac{c_i A_i}{\rho_i}} \tag{3}$$

where A_i and ρ_i are the atomic weight and density of element i. The ρ_i values of elements [5] and calculated ρ_{theor} values for two studied alloys are given in Table 2. It can be seen that the experimentally determined density of Alloy 1 is about 0.8% higher, while that of Alloy 2 is the same as the corresponding calculated densities. These density results are in agreement with the

results of X-ray analysis and support our suggestion that some solution ordering may be present in Alloy 1, while Alloy 2 seems to be a fully disordered solid solution.

Microstructure

SEM backscatter electron images of the refractory alloys are shown in Figures 2 and 3. Large grains of about 200 μm in diameter are observed in the quaternary Alloy 1 (see Figure 2). Uneven Z-contrast inside the grains indicates slightly different compositions of dendritic and interdendritic regions due to constitutional separation during solidification. The quiternary Alloy 2 has a much finer grain structure (see Figure 3). The grain size is about 80 μm and dendrite arms inside the grains are clearly seen. Their lighter Z-contrast indicates that the dendrite arms are enriched with heavier elements than the interdendrite regions. The thickness of the dendrite arms was about the same in both alloys, ~ 20-30 μm. Intergranular and transgranular pores can be seen in both alloys. By excluding these pores, a slightly higher, than experimentally determined, alloy density is expected.

EPMA Analysis

The EPMA analysis was used to determine the level of element segregation between the dendrite arms and interdendritic regions. For this analysis, the elemental compositions were collected at different points along the lines drawn through the grains and dendrites at a spatial resolution of 2 μm. In total, 542 points were analyzed for Alloy 1 and 512 points for Alloy 2. Figure 4 shows the sample regions used for the EPMA analysis. The results are graphically shown in Figure 5 and Figure 6 for Alloy 1 and Alloy 2, respectively. The average, minimum and maximum concentrations of the elements determined by EPMA in these two alloys are given in Table 4 and Table 5, respectively. The average concentrations in the centers of dendrite arms and inter-dendrite regions are also given in these tables. It can be noticed that the distribution of the elements in the alloys is non-homogeneous.

In Alloy 1, the dendrite arms are enriched with W and depleted with Nb and Mo, while the inter-dendritic regions are enriched with Nb and Mo and depleted with W. The concentration of Ta is nearly the same in these regions and is equal to the average concentration. Addition of V in Alloy 2 not only leads to a finer grain structure, but also changes distribution of other elements between the dendrite arms and interdendritic regions. For example, W and Ta become more

segregated and their concentrations in the interdendritic regions are considerably smaller (by 7.3 and 2.0 at.%, respectively) than the average concentration (see Table 5 and Figure 6). In contrast, Mo is distributed more evenly in Alloy 2 than in Alloy1, while the level of segregation of Nb between dendrite arms and interdendritic regions is practically not affected by addition of V. The average concentrations of the elements determined by the EPMA analysis along several lines are slightly different from the values obtained by the ICP-OES analysis (compare Table 1 with Table 4 and Table 5). This is evidently due to the element segregation and different volumes of the alloys used in these two methods.

Microhardness

Vickers microhardness H_v of both alloys was measured in ten randomly selected locations and the results are tabulated in Table 3. The average values of H_v are 4455 MPa and 5250 MPa for the W-Nb-Mo-Ta and W-Nb-Mo-Ta-V alloys, respectively. Alloy 2 has a higher H_v scatter ($\Delta H_v = \pm 281$ MPa) around the average value than Alloy 1 ($\Delta H_v = \pm 185$ MPa) The higher microhardness in Alloy2 is probably due to a finer grain structure, while the larger scatter is due to stronger element segregation. Using an approximate relationship between H_v and the tensile strength σ: $\sigma = H_v/3$, one can estimate $\sigma = 1485 \pm 62$ MPa for W-Nb-Mo-Ta and $\sigma = 1750 \pm 94$ MPa for W-Nb-Mo-Ta-V.

The microhardness of the alloys does not follow the rule of mixture. Indeed, Table 2 shows H_v values for pure elements, which are much smaller than the H_v values for the produced alloys. The rule of mixture $(H_v)_{alloy} = \sum c_i (H_v)_i$ gives the calculated H_v values of 1841 MPa and 1596 MPa for Alloy 1 and Alloy 2, respectively (see Table 2).

CONCLUSIONS

Two single-phase refractory high-entropy alloys, W-Nb-Mo-Ta and W-Nb-Mo-Ta-V, were successfully produced by vacuum arc melting. By definition, the alloys had near-equiatomic compositions. Both alloys had a body centered cubic structure. The lattice parameter, density and microhardness of the W-Nb-Mo-Ta alloy were determined to be $a = 3.2134$ Å, $\rho = 13.75 \pm 0.01$ g/cc and $H_v = 4455 \pm 185$ MPa, respectively. The W-Nb-Mo-Ta-V alloy had $a = 3.1832$ Å, $\rho = 12.36 \pm 0.01$ g/cc and $H_v = 5250 \pm 281$ MPa. The lattice parameter and the density of the quiternary alloy followed the rule of mixture of pure elements indicating fully disordered solid solution.

However, the lattice parameter was smaller and the density was slightly larger than those predicted from the rule of mixture for the quaternary alloy, which was thought to be an indication of some ordering. The Vickers microhardness of the alloys was much higher than the microhardness of pure elements.

The alloys had near-equiaxed dendritic grain structure. The grain size was about 200 μm and 80 μm in the quaternary and quiternary alloys, respectively, while the thickness of the dendrite arms was about the same ~ 20-30 μm. Different concentration of alloying elements inside the dendrite arms and the interdendritic regions was noticed and quantitatively analyzed. In the quaternary alloy, the dendrite arms were enriched with W and Mo and depleted with Nb. In the quiternary alloy, the dendrite arms were enriched with W and Ta and depleted with Nb and V.

ACKNOWLEDGEMENTS

Table 1. Chemical composition (in wt.% / at.%) of two refractory alloys produced by vacuum arc melting.

Alloy ID / Element	W	Nb	Mo	Ta	V
Alloy 1	36.0 / 27.3	15.2 / 22.7	17.8 /25.6	31.7 / 24.4	0.0 / 0.0
Alloy 2	33.0 / 21.1	16.2 / 20.6	17.6 / 21.7	23.9 / 15.6	9.08 / 21.0

Table 2. The crystal lattice parameter, a, density, ρ, and Vickers hardness, H_v, of high purity W, Nb, Mo, Ta and V metals, and two developmental alloys.

Metal	W	Nb	Mo	Ta	V	Alloy 1 Calc	Alloy 1 Exp	Alloy2 Calc	Alloy 2 Exp
a, Å	3.158	3.301	3.1468	3.303	3.039	3.2230	3.2134	3.1827	3.1832
ρ, g/cm^3	19.25	8.57	10.28	16.65	6.11	13.64	13.75	12.36	12.36
H_v, MPa	3430	1320	1530	873	628	1841	4455	1596	5250

Table 3. Vickers microhardness values in ten randomly selected regions of two refractory high entropy alloys.

Alloy/Location	1	2	3	4	5	6	7	8	9	10	Average
WNbMoTa	4547	4398	4332	4418	4547	4537	4626	4379	4256	4507	4455
WNbMoTaV	4857	5405	5378	5225	5126	5263	5353	5237	5237	5418	5250

Table 4. Average, C_{aver}, minimum, C_{min}, and maximum, C_{max}, concentrations of elements in Alloy 1 along four selected lines shown in Figure 4 (a). The average concentrations at the centers of dendrite arms, C_{da}, and inter-dendrite regions, C_{idr}, as well as comparison of these values with C_{aver}, are also given.

| Concentrations (At.%)	Nb	Mo	Ta	W
Average, C_{aver}	24.8	24.0	24.8	26.4
Minimum, C_{min}	20.7	21.7	23.1	18.2
Maximum, C_{max}	30.9	27.8	25.6	31.8
C_{max} - C_{min}	10.1	6.1	2.4	13.6
Average at the center of dendrite arms, C_{CDA}	22.3	22.3	25.1	30.3
C_{da} - C_{aver}	-2.5	-1.7	0.3	3.9
Average in inter-dendrite regions, C_{IDR}	26.8	25.3	24.6	23.3
C_{idr} - C_{aver}	2.0	1.3	-0.2	-3.1

Table 5. Average, C_{aver}, minimum, C_{min}, and maximum, C_{max}, concentrations of elements in Alloy 2 along four selected lines shown in Figure 4 (a). The average concentrations at the centers of dendrite arms, C_{da}, and inter-dendrite regions, C_{idr}, as well as comparison of these values with C_{aver}, are also given.

Concentrations (At.%)	Nb	Mo	Ta	W	V
Average, C_{aver}	20.9	19.1	18.0	22.1	20.0
Minimum, C_{min}	17.5	16.0	12.0	7.3	13.9
Maximum, C_{max}	26.3	20.4	19.9	30.6	38.5
C_{max} - C_{min}	8.8	4.4	8.0	23.3	24.6
Average at the center of dendrite arms, C_{CDA}	19.2	19.0	19.1	26.7	16.0
C_{da} - C_{aver}	-1.7	-0.2	1.1	4.7	-4.0
Average in inter-dendrite regions, C_{IDR}	23.5	19.5	16.0	14.7	26.3
C_{idr} - C_{aver}	2.6	0.4	-2.0	-7.3	6.3
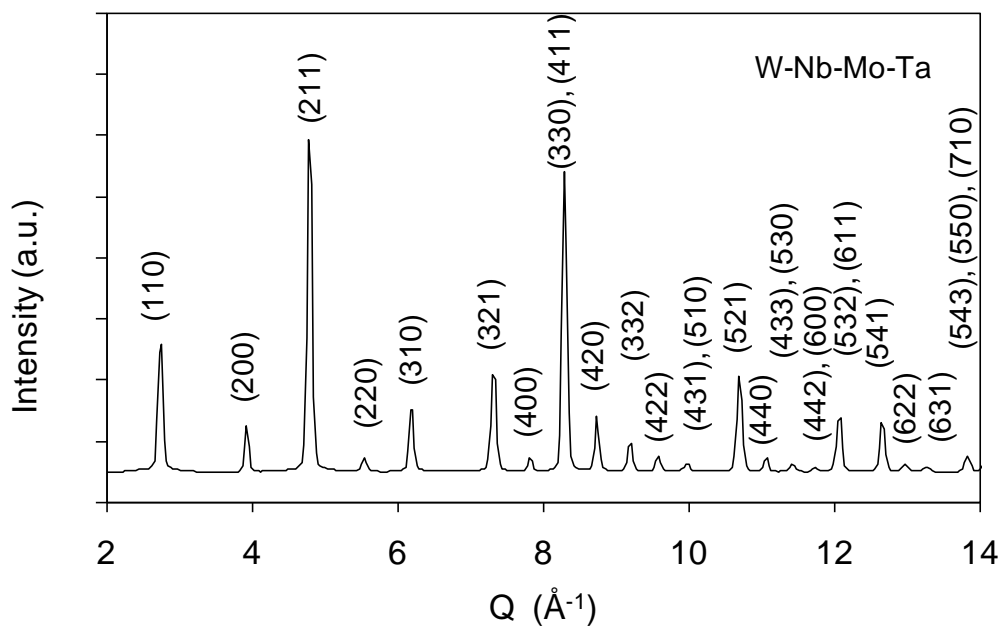
(a)
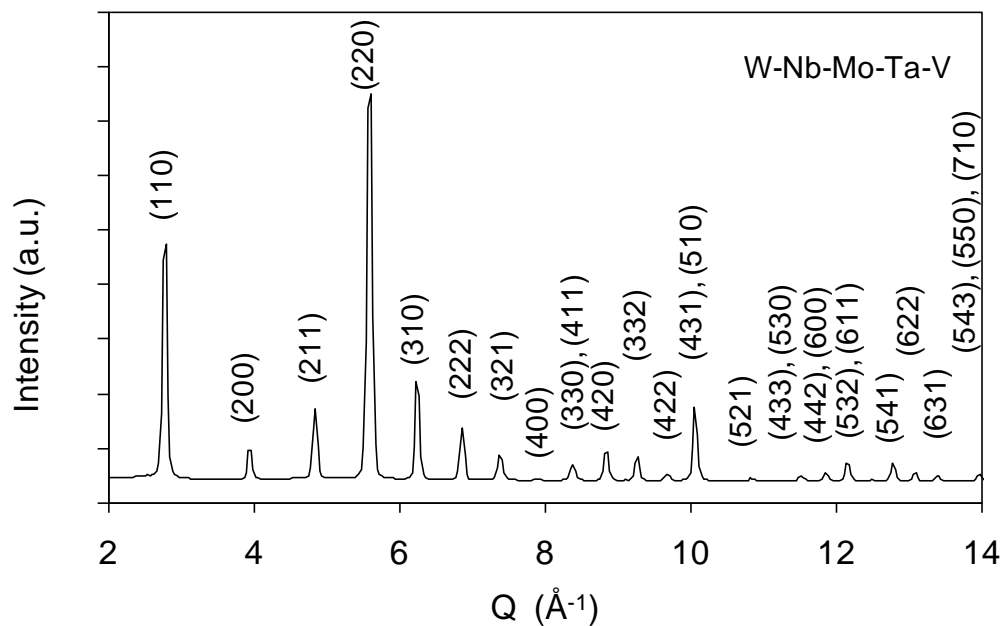
(b)

Figure 1. X-ray diffraction patterns of the (a) W-Nb-Mo-Ta and (b) W-Nb-Mo-Ta-V alloys. All peaks in the patterns belong to the same BCC crystal lattice and their indexes are shown.
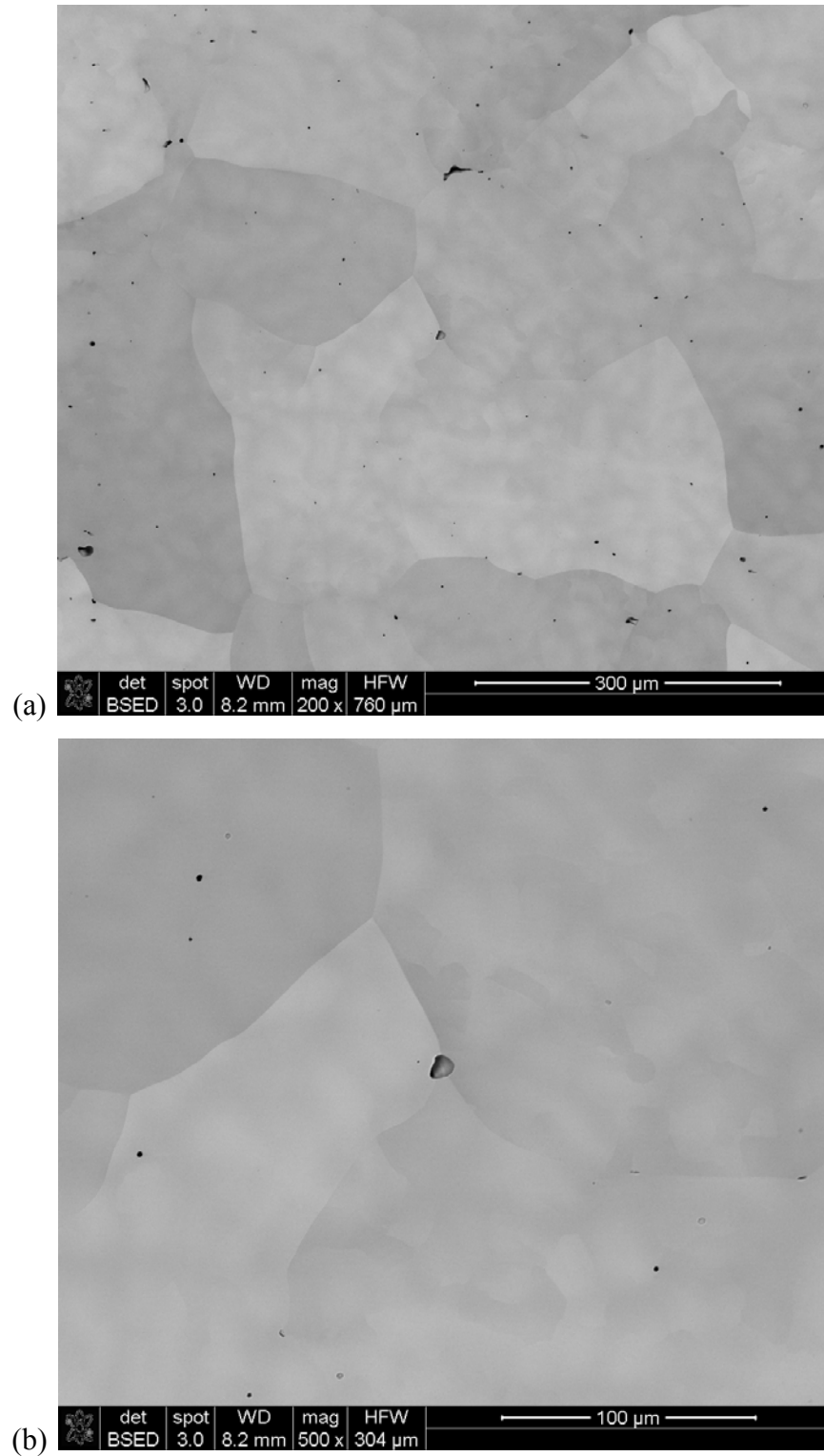
(a)

(b)

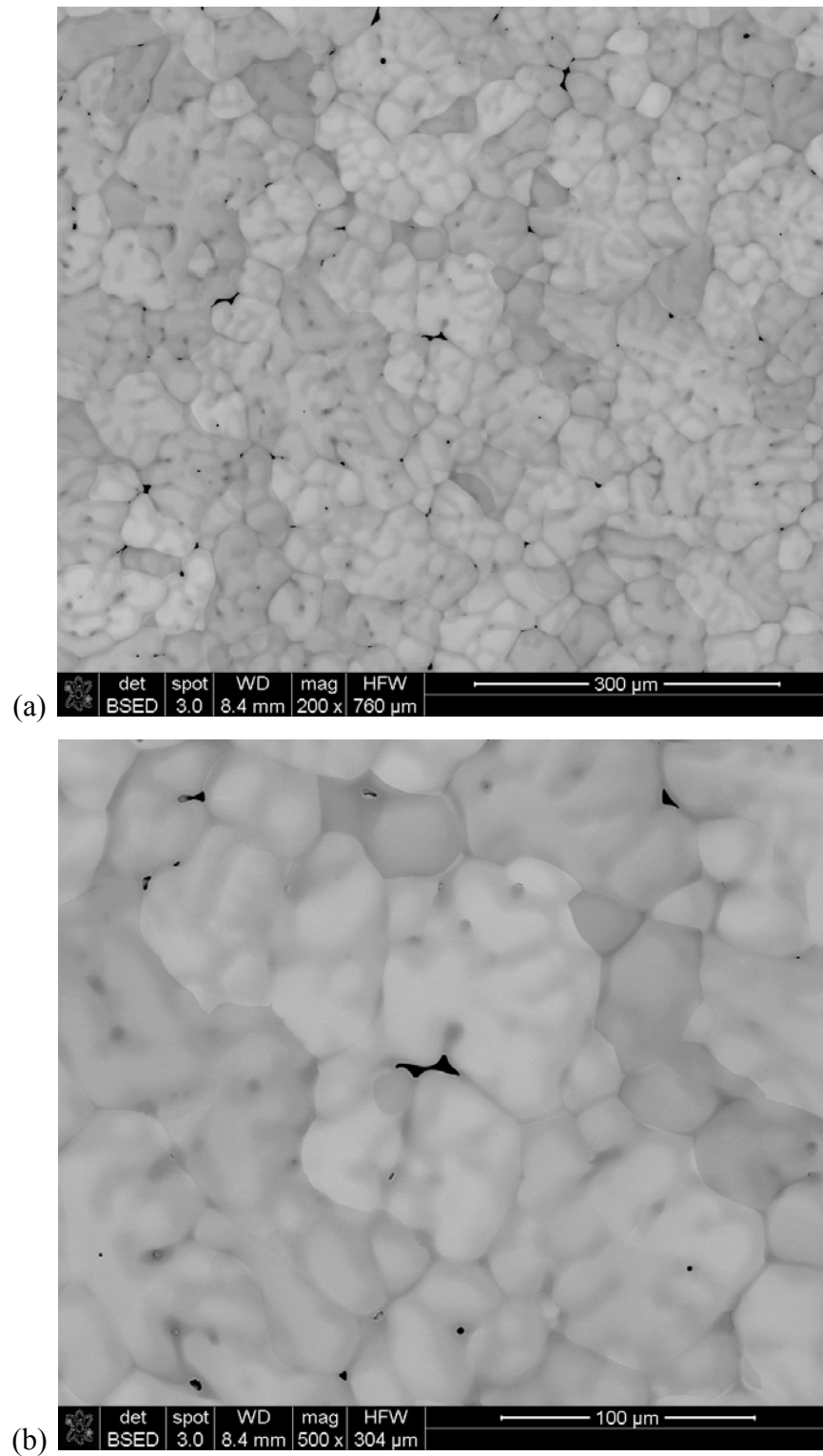Figure 2. SEM backscatter electron images of a polished cross-section of W-Nb-Mo-Ta alloy taken at two different magnifications..

(a)

(b)

Figure 3. SEM backscatter electron images of a polished cross-section of W-Nb-Mo-Ta-V alloy taken at two different magnifications.
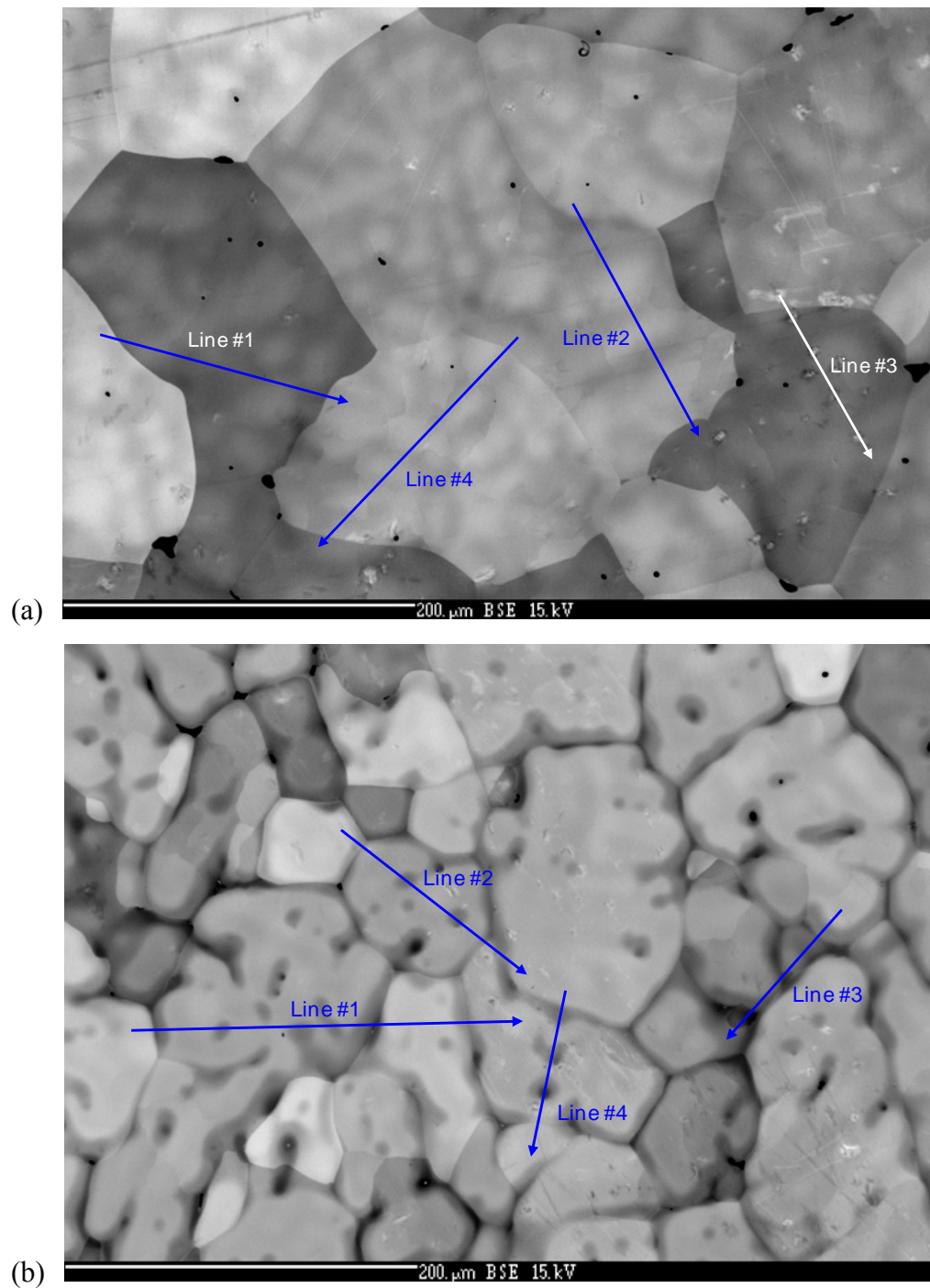
Figure 4. SEM backscatter electron images of the regions of (a) Alloy 1 and (b) Alloy 2 from which the EPMA analysis was conducted. The elemental composition gradients were determined along the drawn lines with the spacious resolution of 2 μm.
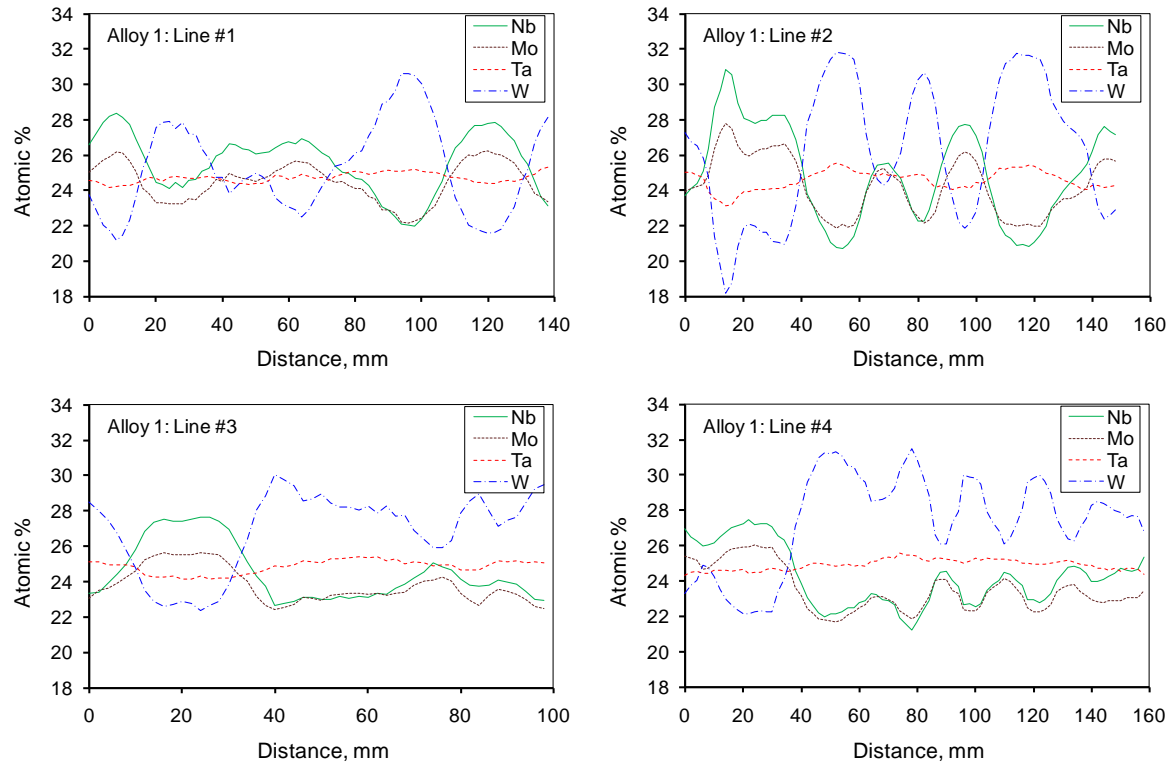
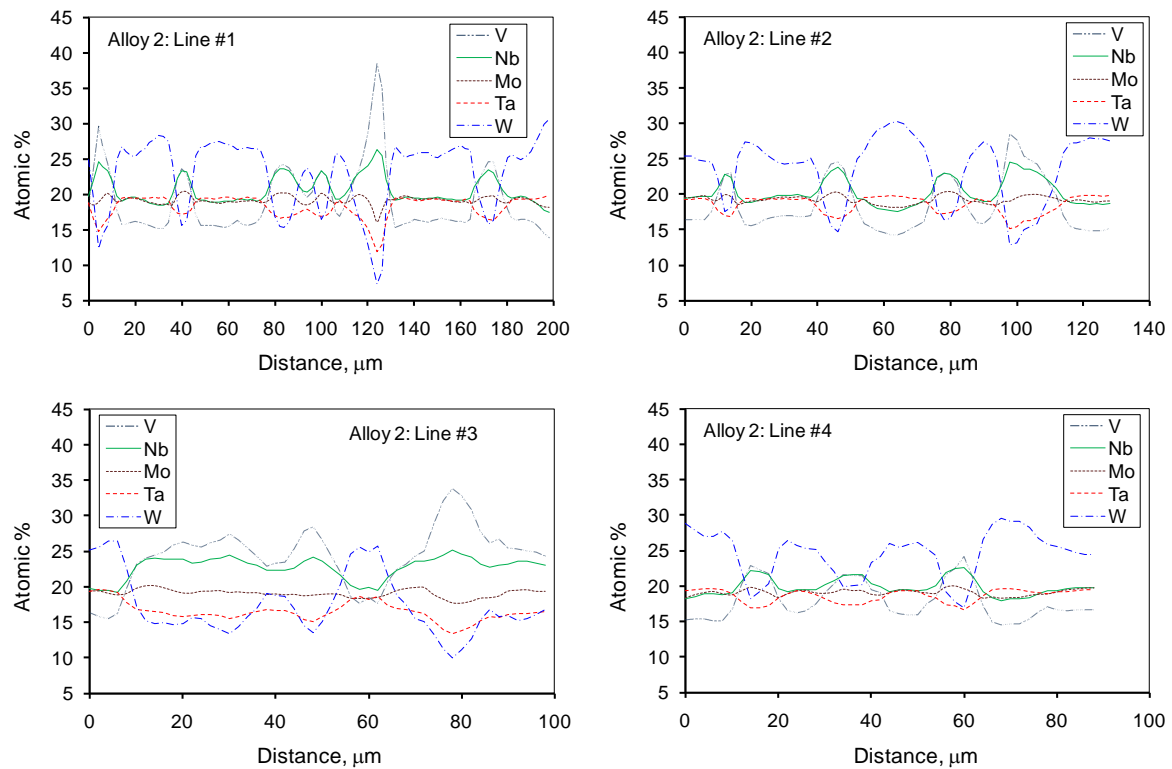Figure 5. Distribution of elements in Alloy 1 along the lines shown in Figure 4 (a).

Figure 6. Distribution of elements in Alloy 2 along the lines shown in Figure 4 (b).

REFERENCES

1 Yeh, J.W., et al., Nanostructured high-entropy alloys with multiple principal elements: Novel alloys design concepts and outcomes. Adv. Eng. Mater., 2004. 6(5): p. 299-303.

2 Huang, P.K., J.W. Yeh, T.T. Shun, and S.K. Chen, Multi-principal-element alloys with improved oxidation and wear resistance for thermal spray coating. Adv. Eng. Mater., 2004. **6**(1-2): p. 74-78.

3 Yeh, J.W., Recent progress in high entropy alloys. Ann. Chim. Sci. Mat., 2006. **31**(6): p. 633-648.

4 International Tables for X-ray Crystallography, Birmingham, England, 1968.

5 WebElements: http://www.webelements.com/periodicity/density.